Published in final edited form as:
J Am Coll Cardiol. 2010 August 10; 56(7): 561–569. doi:10.1016/j.jacc.2010.02.061.

Assessment of Advanced Coronary Artery Disease:

Advantages of Quantitative Cardiac Magnetic Resonance Perfusion Analysis

Amit R. Patel, MD[*], **Patrick F. Antkowiak, BS**[†], **Kiran R. Nandalur, MD**[||], **Amy M. West, MD**[‡], **Michael Salerno, MD, PhD**[‡], **Vishal Arora, MD**[¶], **John Christopher, RT**[§], **Frederick H. Epstein, PhD**[†,§], and **Christopher M. Kramer, MD**[‡,§]

[*] Department of Medicine, University of Chicago, Chicago, Illinois

[†] Department of Biomedical Engineering, University of Virginia, Charlottesville, Virginia

[‡] Department of Medicine, University of Virginia, Charlottesville, Virginia

[§] Department of Radiology, University of Virginia, Charlottesville, Virginia

[||] Department of Radiology, William Beaumont Hospital, Royal Oak, Michigan

[¶] Department of Medicine, Medical College of Georgia, Augusta, Georgia

Abstract

Objectives—The purpose of this paper was to compare quantitative cardiac magnetic resonance (CMR) first-pass contrast-enhanced perfusion imaging to qualitative interpretation for determining the presence and severity of coronary artery disease (CAD).

Background—Adenosine CMR can detect CAD by measuring perfusion reserve (PR) or by qualitative interpretation (QI).

Methods—Forty-one patients with an abnormal nuclear stress scheduled for X-ray angiography underwent dual-bolus adenosine CMR. Segmental myocardial perfusion analyzed using both QI and PR by Fermi function deconvolution was compared to quantitative coronary angiography.

Results—In the 30 patients with complete quantitative data, PR (mean ± SD) decreased stepwise as coronary artery stenosis (CAS) severity increased: 2.42 ± 0.94 for <50%, 2.14 ± 0.87 for 50% to 70%, and 1.85 ± 0.77 for > 70% ($p < 0.001$). The PR and QI had similar diagnostic accuracies for detection of CAS > 50% (83% vs. 80%), and CAS > 70% (77% vs. 67%). Agreement between observers was higher for quantitative analysis than for qualitative analysis. Using PR, patients with triple-vessel CAD had a higher burden of detectable ischemia than patients with single-vessel CAD (60% vs. 25%; $p = 0.02$), whereas no difference was detected by QI (31% vs. 21%; $p = 0.26$). In segments with myocardial scar (n = 64), PR was 3.10 ± 1.34 for patients with CAS <50% (n = 18) and 1.91 ± 0.96 for CAS >50% ($p < 0.0001$).

Conclusions—Quantitative PR by CMR differentiates moderate from severe stenoses in patients with known or suspected CAD. The PR analysis differentiates triple- from single-vessel CAD, whereas QI does not, and determines the severity of CAS subtending myocardial scar. This has important implications for assessment of prognosis and therapeutic decision making.

Keywords

myocardial perfusion imaging; MRI; ischemia; coronary artery disease; perfusion reserve; perfusion

Reprint requests and correspondence: Dr. Christopher M. Kramer, University of Virginia Health System, Departments of Medicine and Radiology, 1215 Lee Street, Box 800170, Charlottesville, Virginia 22908. ckramer@virginia.edu.
Drs. Patel, Antkowiak, Epstein, and Kramer contributed equally to this work.

Cardiac magnetic resonance (CMR) perfusion imaging is an important clinical tool for the detection of significant coronary artery disease (CAD) (1,2). Image analysis can be performed using qualitative interpretation (QI), in which a hypointense segment seen during the initial transit of a contrast agent through the myocardium during hyperemic conditions represents ischemia. When combined with myocardial scar imaging, in 1 recent study, first-pass perfusion imaging using QI had a sensitivity and specificity of 89% and 87%, respectively, for the detection of CAD (3). Also using QI, another study showed that the absence of ischemia on a perfusion CMR study identifies a group of patients who have a <1% likelihood of having a cardiac event during the subsequent 3 years (4).

A potential advantage of perfusion CMR is its ability to quantify perfusion reserve (PR) within a myocardial segment. Semiquantitative estimates of PR such as the upslope index have been validated against invasive fractional flow reserve in a highly selective patient population (5), but when compared to positron emission tomography, it is apparent that the upslope index was not an adequate surrogate of PR at higher myocardial blood flows (6). Regardless, in a recent study, the presence of an abnormal regional semiquantitative perfusion reserve index had a sensitivity and specificity of 88% and 90%, respectively, for the detection of significant CAD (7). More quantitative measurements of PR determined by de-convolution of the tissue function (TF) and the arterial input function (AIF) require low doses of contrast, which limits signal-to-noise ratio in the tissue and can weaken qualitative analysis (8). However, in 1 study, when compared to invasive fractional flow reserve and X-ray angiography, the presence of an abnormal quantitative measurement of PR still had a relatively poor specificity for detecting significant CAD (9), possibly due to error introduced by inadequate estimation of the TF. Recently, a newer quantitative technique, in which the AIF and TF are acquired during separate boluses of gadolinium-diethylenetriamine penta-acetic acid (Gd-DTPA), has been shown to correlate very precisely with absolute myocardial blood flow over the full range of physiologic flow values (10). The advantage of this technique is that the AIF is accurately measured using the low-dose contrast bolus, and the TF is measured, either quantitatively or qualitatively, with high signal-to-noise ratio using a high-dose contrast bolus.

Potential benefits of measuring PR include reduced interpreter bias, quantification of treatment response, and improved detection of balanced ischemia. Despite these potential benefits, quantitative PR analysis is time consuming and has not been adopted in clinical practice. No prospective comparisons of QI and quantitative PR analysis have been performed to date. We sought to determine whether PR analysis provides additional clinically relevant information when compared to QI. We hypothesized that PR analysis would improve the assessment of severe and triple-vessel CAD.

Methods

Population

We recruited 41 patients with an abnormal single-positron emission computed tomography stress test who were awaiting or had undergone a diagnostic X-ray angiogram (within 30 days without intervention or clinical events) as part of their clinical care. Patients were excluded if they had a recent myocardial infarction, were older than 85 years, or had any contraindications to CMR or adenosine. Patients were asked to avoid beta-blockers, nitrates, and caffeine before their stress CMR study. The institutional review board approved the study protocol, and all patients provided informed consent.

CMR protocol

All CMR studies were performed on either a Sonata or Avanto MRI 1.5-T scanner (Siemens Healthcare, Erlangen, Germany) with a 4-channel phased array radiofrequency coil.

DUAL-BOLUS STRESS PERFUSION CMR—Before the infusion of adenosine or contrast agent, 3 short-axis slices of the left ventricle (base, mid, and apex) were acquired as localizers using a hybrid gradient echo and echo-planar imaging pulse sequence (GRE-EPI) (11): nonselective 90° saturation pulse followed by an 80 ms delay, field of view = 340 to 400 × 212 to 360 mm, matrix = 128 × 80, slice thickness = 8 mm, flip angle = 25°, repetition time (TR) = 5.6 to 6.2 ms, echo time (TE) = 1.3 ms, echo train length = 4, effective spatial resolution approximately 2.8 × 2.8 mm with (n = 23) or without (n = 18) rate 2 parallel imaging (TSENSE) (12). Adenosine (Adenoscan, Astellas, Tokyo, Japan) 140 μg/kg/min was then infused. After 2 to 3 min of infusion, a low dose of Gd-DTPA (Magnevist, Bayer Healthcare, Leverkusen, Germany; 0.0075 mmol/kg at 4 ml/s) was injected to measure the AIF and was immediately followed by a higher dose of Gd-DTPA (0.075 mmol/kg) to measure the TF. Each infusion was followed by 20 ml normal saline (4 ml/s). The GRE-EPI images were acquired during the first pass of both the low-dose and higher-dose Gd-DTPA infusions for 40 to 50 heartbeats each. An image of each of the 3 short-axis slices was acquired during each heartbeat. After perfusion imaging, the adenosine was discontinued.

CINE CMR—Steady-state free precession imaging (TR/TE 3 ms/1.1 to 1.3 ms) was used to obtain cine images of the left ventricle in the short-axis plane (8-mm slice thickness with 20% gap) and in 2-, 3-, and 4-chamber long-axis views.

REST PERFUSION CMR—Ten minutes after stopping adenosine, first-pass perfusion imaging with both low- and higher-dose Gd-DTPA was repeated under resting conditions.

LATE GADOLINIUM ENHANCEMENT—Five minutes after rest perfusion imaging, late gadolinium enhancement imaging was performed in the same slices to detect the presence of myocardial scar using either T1-weighted inversion recovery GRE (inversion time [TI] based on optimal nulling of the myocardium, TR 750 ms, TE 4.3 ms, flip angle = 30°) or phase-sensitive inversion recovery GRE (TR 700 ms, TE 4.2 ms, TI 300 ms, flip angle = 25°).

Qualitative CMR interpretation

The QI was performed separately by 2 highly experienced interpreters (with American College of Cardiology Foundation/American Heart Association [AHA] Level 3 CMR clinical competence and training) blinded to all clinical and X-ray angiography data. The presence or absence of a perfusion defect was assigned to the appropriate segment of a modified AHA 16-segment model. A perfusion defect was considered to be positive if it was present after peak contrast enhancement of the LV cavity and persisted for several beats. Figure 1 shows a large perfusion defect in the basal, mid-ventricular, and apical slices during hyperemia but not during resting conditions.

Quantitative CMR analysis

The PR quantification was performed using Fermi function deconvolution (8,13). Convolution of the AIF with a flow-weighted residue function (whose initial amplitude is a measure of myocardial perfusion) yields the TF; thus, perfusion can be calculated through deconvolution of the AIF from the TF. A large region of interest was drawn using Argus software (Siemens Medical Solutions, Munich, Germany) in the basal slice of the left ventricular cavity of the low-dose Gd-DTPA perfusion images to generate time-intensity curves representing the AIF; similarly, the endocardial and epicardial surfaces were manually delineated on the higher dose Gd-DTPA perfusion images, and the 16-segment model was applied. The subendocardial (and also the subepicardial) halves of these segments were used to generate time intensity curves representing the TFs. All curves were resampled into 1-s intervals, and the AIF was scaled by a factor of 10 to account for the gadolinium dose and fit to a gamma-variate function.

Constrained Fermi function deconvolution was then performed using custom software developed in MATLAB (The Mathworks, Inc., Natick, Massachusetts). For the deconvolution procedure, approximately 20 s to 25 s of the AIF and TF were selected for analysis, which included both pre-contrast points as well as points several seconds after peak contrast enhancement. The user adjusted a delay parameter to align the AIF and TF, since they were not acquired simultaneously. A Marquardt-Levenberg nonlinear least squares optimization algorithm was used to estimate the 3 parameters describing the Fermi function. The initial amplitude of the Fermi function was recorded as the perfusion measurement. This perfusion measurement was made in units of $minute^{-1}$, and was not scaled to be in units of ml/g/min. Thus, this measurement is not suitable for direct assessment of tissue perfusion, but is perfectly suitable for calculation of PR.

The PR, defined as the ratio of stress to rest perfusion, was determined for each segment. In addition, the transmural gradient (or endocardial to epicardial blood flow ratio [ENDO/EPI]) during stress perfusion was determined for each segment. Figure 2 shows a typical AIF and example TFs for segments supplied by a normal coronary artery and a stenosed coronary artery. A subset of 10 studies was reanalyzed separately by a second blinded person to determine the interobserver variability of PR quantification.

Angiographic analysis

The X-ray angiography was performed using standard clinical techniques and interpreted by an interventional cardiologist blinded to all clinical and CMR data. Quantitative coronary angiography was used to categorize stenoses as <50%, 50% to 70%, or >70%. All stenoses were then assigned to the appropriate segment of a modified AHA 16-segment model.

Statistical analysis

Analysis was performed using Prism (GraphPad Software, San Diego, California). Continuous variables are expressed as mean ± SD and were compared using unpaired *t* tests. Receiver-operating characteristic curve analysis was used to determine optimal PR cutoff values (defined as the PR value that resulted in the highest diagnostic accuracy). Sensitivities and specificities were determined for both qualitative and quantitative analyses and compared using the McNemar test. The Kruskal-Wallis 1-way analysis of variance by ranks with a post-test was used to compare the relationship (and any trends that exist) between PR and severity of coronary artery stenosis (CAS). A p value <0.05 was considered statistically significant. Interobserver agreement was measured using kappa statistics.

Results

Study population

Forty-one patients were enrolled in the study (32% female, mean age 68 ± 12 years). Patient characteristics are described in Table 1. The typical patient was obese (body mass index 30.2 ± 4.8 kg/m^2) and hypertensive. The X-ray angiography demonstrated significant CAD in 71%. Thirty-seven percent of the total population had 3-vessel CAD, and 27% had 1-vessel CAD. Left ventricular size and function are shown in Table 1. By late gadolinium enhancement, 44% had a prior myocardial infarction. One patient refused X-ray angiography and another was excluded from analysis because his chest pain was a result of acute myocarditis. Of the remaining 39 patients, 30 patients had adequate data for PR analysis. The 23% of quantitative data sets that were incomplete were due to inadequate clearance of Gd-DTPA before acquisition of the resting AIF (n = 3), image acquisition error (n = 3), insufficient contrast dose during stress AIF (n = 2), or poor image quality (n = 1). Most of these occurred in the earlier studies and occurred at a lower frequency as we gained experience with the technique.

PR analysis

A stepwise reduction in PR occurred as the severity of coronary stenosis increased (Fig. 3). Specifically, PR was 2.42 ± 0.94 in myocardial segments perfused by CAS <50% (n = 245), 2.14 ± 0.87 for CAS 50% to 70% (n = 92), and 1.85 ± 0.77 for CAS >70% (n = 143; $p < 0.001$ for trend). Segments with late gadolinium enhancement (indicating the presence of myocardial scar) that were subtended by a CAS <50% (n = 18) had a preserved PR of 3.10 ± 1.34; whereas those subtended by a CAS >50% (n = 46; 33 of 46 with CAS >70%) had a reduced PR of 1.91 ± 0.96 ($p < 0.0001$). There was no difference in the frequency of transmural and nontransmural scars in segments with or without CAS >50% (data not shown). Additionally, there was no difference in perfusion reserve between segments with a transmural scar (PR = 2.36 ± 1.25) and those with a nontransmural scar (PR = 1.83 ± 0.91, $p = 0.14$). There was no relationship detected between the severity of stenosis and ENDO/EPI under hyperemic or resting conditions. Under hyperemic conditions, ENDO/EPI for CAS <50% was 1.051 ± 0.175; for CAS 50% to 70%, it was 1.053 ± 0.170; and for CAS >70%, it was 1.067 ± 0.373 ($p = 0.39$). Under resting conditions, ENDO/EPI for CAS <50% was 1.131 ± 0.290; for CAS 50% to 70%, it was 1.130 ± 0.207; and for CAS >70%, it was 1.136 ± 0.265 ($p = 0.74$).

Diagnostic performance

In the entire cohort, QI detected patients who had a CAS >50% with a sensitivity of 79%, specificity of 90%, and accuracy of 82%; whereas CAS >70% was detected with a sensitivity, specificity, and accuracy of 77%, 59%, and 69%, respectively. For the 30 patients who successfully completed both QI and PR analysis, QI had a sensitivity, specificity, and accuracy of 79%, 83%, and 80%, respectively, for the detection of CAS >50%. Similar to that seen in the overall group, when QI was used to detect only CAS >70%, the sensitivity was essentially unchanged (78%) while the specificity and accuracy decreased to 50% and 67%.

Because PR is related to the severity of underlying CAS, an optimal PR cutoff value can be selected for the detection of a specific severity of coronary stenosis. Using receiver-operating characteristics, PR analysis had an area under the curve of 0.82 for the detection of CAS >50% and 0.77 for CAS >70%. The optimal PR cutoff value, defined as the PR cutoff value that maximized diagnostic accuracy, for detecting patients with CAS >50% was 1.85; whereas the best cutoff value was 1.55 for detecting those with CAS >70%. The PR analysis detected CAS >50% with a sensitivity, specificity, and diagnostic accuracy of 88%, 67%, and 83%, respectively. The odds ratio that QI and PR analysis were the same for detecting CAS >50% was 2.0 (95% confidence interval: 0.43 to 12.4, p = NS). The accuracy for detecting patients with CAS >70% was 77% for PR and 67% for QI. The sensitivity was 78% for both, but specificity was 75% for QI and 50% for PR; however, these differences were not statistically significant. Segments with a PR of <1.55 tended to have lower wall thickening (47 ± 33%) than did segments with a PR >1.55 (54 ± 41%, $p = 0.09$). The diagnostic performance of PR for detecting CAS >50% or >70% was not improved by normalizing the PR to resting rate pressure product.

Figure 4 represents a patient with multivessel coronary disease that was not detected using QI but was readily identified using PR analysis.

Reproducibility

On a per-patient basis for QI, interobserver agreement was moderate (kappa = 0.54, 95% confidence interval: 0.25 to 0.82) for the detection of CAS >50%. There was better agreement for quantitative PR analysis for the detection of CAS >50% (kappa = 0.66, 95% confidence interval: 0.54 to 0.78).

Evaluation of ischemic burden

As shown in Figure 5, when estimated using QI, the myocardial ischemic burden was similar in patients with triple-vessel CAD (n = 14) and single-vessel (n = 8; 31 ± 20% vs. 21 ± 26%, p = 0.26). When ischemic burden was measured using PR analysis, patients with triple-vessel CAD had more ischemia than patients with single-vessel CAD (60 ± 38% vs. 25 ± 41%, p = 0.02). Figure 6 represents a patient with multivessel CAD who had only a small amount of visually appreciable ischemia, but the PR was severely reduced in the majority of the left ventricle.

Image contrast-to-noise ratio and dispersion of AIF

The myocardial contrast-to-noise ratio (defined as $[SI_{peak} - SI_{pre\text{-}contrast}]/\sigma_{pre\text{-}contrast}$) was calculated for each tissue segment at stress and rest. Contrast-to-noise ratio was 42 ± 13 for the stress studies and 35 ± 14 for the rest studies, with the lower rest value due to the presence of residual gadolinium initially in the myocardium from the prior stress scan. The AIF bolus underwent less dispersion in the stress scan compared with the rest scan, as the full width at half-maximum of the AIF was 7.0 ± 3.0 s for the stress studies compared with 9.3 ± 3.3 s for the rest studies ($p < 0.01$).

Discussion

We used dual-bolus perfusion CMR to determine the relationship between PR and CAS in patients with known or suspected CAD. We observed stepwise decreases in PR as the severity of CAS increased. We also found that PR analysis was better than QI at discriminating patients with triple-vessel CAD from those with only single-vessel CAD. The PR analysis accurately differentiated scarred myocardial segments perfused by significantly stenosed coronary arteries from those that were not. Agreement between observers was higher for quantitative than qualitative analysis.

PR and severity of CAS

Previous studies using positron emission tomography have shown that PR is inversely related to the severity of underlying CAS (14). Myocardial blood flow measured using the dual-bolus perfusion CMR technique (10) is highly correlated to measurements made with gold-standard radiolabeled microspheres. The differentiation of varying degrees of CAS requires a measurement of PR that accurately estimates the full range of clinically relevant myocardial blood flow. The inverse relationship between PR and CAS has been difficult to measure using CMR in patients because commonly used approaches such as the upslope technique do not adequately correlate with myocardial blood flow >2 ml/g/min (10). Techniques such as deconvolution (8,13) can accurately measure myocardial blood flow but were previously applied using low doses of Gd-DTPA, which is suboptimal for QI due to poor contrast-to-noise ratio. The dual-bolus technique uses high enough doses of Gd-DTPA to visually assess and measure tissue perfusion and very low doses of Gd-DTPA to accurately measure the AIF (10). This combination prevents the underestimation of myocardial blood flow without sacrificing the contrast-to-noise ratio needed for optimal QI. Using this CMR technique, we successfully detected the expected stepwise reduction in PR with worsening CAS.

Diagnostic performance

Both QI (2,3,15) and PR analysis (5,7,9) can be used to detect significant CAD, and overall accuracy is similar for stenosis detection. The diagnostic performance of both approaches is dependent on technical factors such as the pulse sequence used and selection of the optimal contrast dose. As demonstrated by the reproducibility analysis performed in our study, the benefits of PR analysis include better interobserver agreement. However, it is time consuming,

and it was previously unknown whether quantification adds substantial clinical benefit for the evaluation of CAD. We show in this prospective, head-to-head comparison of QI and PR that the latter improves the evaluation of 3-vessel CAD.

Although PR analysis performed well in our study, it is known that perfusion is a measurement of the hemodynamic consequences of a CAS (16) and that coronary angiography is an imperfect standard for judging myocardial perfusion imaging. In fact, Pijls et al. (17) have shown using an invasive technique that not all 50% coronary stenoses are hemodynamically significant (17). When compared to fractional flow reserve rather than coronary angiography, perfusion CMR accurately differentiated physiologically significant stenoses >50% from those that were not flow limiting (5). The lower specificity seen in our study was likely due to the patient population studied. Although PR is clearly reduced in patients with a severe CAS, there are other causes of abnormal PR such as hypertension, diabetes mellitus, hyperlipidemia, and cardiac syndrome X (18–22). Eighty-three percent of our population had a history of hypertension, 27% had diabetes mellitus, and 88% had dyslipidemia. In our study, QI had a sensitivity of 79% for detecting CAS >50%. In fact, the example shown in Figure 4 shows a patient with significant 3-vessel CAD who has no visually apparent perfusion defect but has a reduced PR. One potential mechanism for false negative visual interpretation is the presence of balanced transmural ischemia where there are no adequately perfused segments that can be used as a normal reference.

Assessment of left ventricular ischemic burden

Although QI could be used to diagnose the presence of significant CAD, patients with multivessel CAD were not reliably differentiated from patients with only single-vessel disease: no difference in ischemic burden was visually apparent in the 2 groups because QI underestimated the amount of ischemia present in patients with 3-vessel CAD. Conversely, when the ischemic burden was quantified using PR analysis, patients with multivessel CAD had more ischemia than patients with single-vessel CAD. A similar phenomenon has been described using positron emission tomography (23). An accurate assessment of ischemic burden is important because the extent of ischemia is a marker of patient prognosis: patients with lesser amounts of ischemia have a better prognosis than do patients with extensive ischemia (24). Additionally, the ischemic burden can be used to identify patients who may benefit from more aggressive treatment strategies such as revascularization (25). In fact, even asymptomatic patients with extensive ischemia may have better outcomes with revascularization (26). Thus, quantitative analysis may offer improved assessment of patient prognosis and help to identify the optimal therapeutic approach.

PR in segments with myocardial scar

Previous studies demonstrate that in the presence of a myocardial scar, resting myocardial blood flow is inversely related to the transmural extent of scar (27). Additionally, PR is acutely diminished in small scars that occur as a complication of percutaneous coronary intervention (28). However, it was previously unknown whether PR analysis could be used to determine if a scarred segment is subtended by a significantly stenosed coronary artery. Forty-four percent of our study population had evidence of a myocardial scar. In myocardial segments with a scar, the PR was significantly lower if the segment was supplied by a stenosed coronary artery. Therefore, our data suggest that PR can be used to detect the presence or absence of hemodynamically significant CAD in patients with a history of prior myocardial infarction.

Study limitations

Our sample size is small, and both patient selection bias and test verification bias are likely present. Also, quantification was time consuming (approximately 30 to 45 min per study) and was unable to be performed in 23% of the studies. Our study will need to be confirmed in future

larger trials using the dual-bolus PR analysis. Because the dual-bolus technique requires 4 separate injections of Gd-DTPA, a technical problem during any 1 of the 4 injections affects the composite measurement of PR. This is an important limitation of the dual-bolus approach and may reduce its clinical applicability. However, with a learning curve, very few problems were encountered during the latter half of the study. Newer dual-contrast pulse sequences that require only 2 injections will simplify the procedure (29). The imaging protocol used in this study included only a 10-min delay between stress and rest perfusion imaging. This resulted in inadequate data quality for perfusion reserve analysis in 3 patients. It may be prudent to wait longer before rest imaging. For our gadolinium injections, the volumes of the AIF bolus and TF bolus were not identical. Ideally, the low AIF doses should have been diluted into volumes equivalent to that used for the TF. However, the same AIF volumes were used for the stress and rest scans, and any systematic error resulting from the small AIF volumes would mostly cancel out when dividing to calculate the perfusion reserve. Additionally, our study was performed using a 1.5-T MRI scanner; it is likely that imaging at 3.0-T could have improved our results (30).

Conclusions

We have shown in this prospective, head-to-head comparison that PR analysis of first-pass CMR images provides additional clinically relevant information compared with QI. Specifically, compared with QI, quantification of PR can differentiate moderate from severe CAD and can better discriminate patients with triple-vessel CAD from patients with single-vessel CAD. Additionally, PR analysis can be used to differentiate scarred myocardial segments that are supplied by a severely stenosed coronary artery from those that are not. Agreement between observers is better for quantitative analysis. Thus, continued technical development to automate PR analysis is warranted. These findings have important implications for ascertaining prognosis in an individual patient and determining an optimal therapeutic approach.

Acknowledgments

This study was supported in part by research grants from Astellas Pharma US Inc., Siemens Medical Solutions, and 5-T32 EB003841. Dr. Patel has received a research grant from Astellas Pharma. Dr. Epstein has received research support from Siemens Medical Solutions. Dr. Kramer has received research equipment support from Siemens Medical Solutions and a research grant from Astellas Pharma. Mr. Antkowiak and Drs. Nandalur, West, Salerno, Arora, and Christopher have reported that they have no relationships to disclose.

Abbreviations and Acronyms

AIF	arterial input function
CAD	coronary artery disease
CAS	coronary artery stenosis
CMR	cardiac magnetic resonance
ENDO/EPI	endocardial to epicardial blood flow ratio
Gd-DTPA	gadolinium-diethylenetriamine penta-acetic acid
GRE-EPI	hybrid gradient echo/echo planar imaging
PR	perfusion reserve
QI	qualitative interpretation
TE	echo time

TF	tissue function
TI	inversion time
TR	repetition time

References

1. Nandalur KR, Dwamena BA, Choudhri AF, Nandalur MR, Carlos RC. Diagnostic performance of stress cardiac magnetic resonance imaging in the detection of coronary artery disease: a meta-analysis. J Am Coll Cardiol 2007;50:1343–53. [PubMed: 17903634]
2. Schwitter J, Wacker CM, van Rossum AC, et al. MR-IMPACT: comparison of perfusion-cardiac magnetic resonance with single-photon emission computed tomography for the detection of coronary artery disease in a multicentre, multivendor, randomized trial. Eur Heart J 2008;29:480–9. [PubMed: 18208849]
3. Klem I, Heitner JF, Shah DJ, et al. Improved detection of coronary artery disease by stress perfusion cardiovascular magnetic resonance with the use of delayed enhancement infarction imaging. J Am Coll Cardiol 2006;47:1630–8. [PubMed: 16631001]
4. Jahnke C, Nagel E, Gebker R, et al. Prognostic value of cardiac magnetic resonance stress tests: adenosine stress perfusion and dobut-amine stress wall motion imaging. Circulation 2007;115:1769–76. [PubMed: 17353441]
5. Rieber J, Huber A, Erhard I, et al. Cardiac magnetic resonance perfusion imaging for the functional assessment of coronary artery disease: a comparison with coronary angiography and fractional flow reserve. Eur Heart J 2006;27:1465–71. [PubMed: 16720685]
6. Ibrahim T, Nekolla SG, Schreiber K, et al. Assessment of coronary flow reserve: comparison between contrast-enhanced magnetic resonance imaging and positron emission tomography. J Am Coll Cardiol 2002;39:864–70. [PubMed: 11869854]
7. Nagel E, Klein C, Paetsch I, et al. Magnetic resonance perfusion measurements for the noninvasive detection of coronary artery disease. Circulation 2003;108:432–7. [PubMed: 12860910]
8. Jerosch-Herold M, Wilke N, Stillman AE. Magnetic resonance quantification of the myocardial perfusion reserve with a Fermi function model for constrained deconvolution. Med Phys 1998;25:73–84. [PubMed: 9472829]
9. Costa MA, Shoemaker S, Futamatsu H, et al. Quantitative magnetic resonance perfusion imaging detects anatomic and physiologic coronary artery disease as measured by coronary angiography and fractional flow reserve. J Am Coll Cardiol 2007;50:514–22. [PubMed: 17678734]
10. Christian TF, Rettmann DW, Aletras AH, et al. Absolute myocardial perfusion in canines measured by using dual-bolus first-pass MR imaging. Radiology 2004;232:677–84. [PubMed: 15284436]
11. Ding S, Wolff SD, Epstein FH. Improved coverage in dynamic contrast-enhanced cardiac MRI using interleaved gradient-echo EPI. Magn Reson Med 1998;39:514–9. [PubMed: 9543412]
12. Kellman P, Epstein FH, McVeigh ER. Adaptive sensitivity encoding incorporating temporal filtering (TSENSE). Magn Reson Med 2001;45:846–52. [PubMed: 11323811]
13. Axel L. Tissue mean transit time from dynamic computed tomography by a simple deconvolution technique. Invest Radiol 1983;18:94–9. [PubMed: 6832937]
14. Uren NG, Melin JA, De Bruyne B, Wijns W, Baudhuin T, Camici PG. Relation between myocardial blood flow and the severity of coronary-artery stenosis. N Engl J Med 1994;330:1782–8. [PubMed: 8190154]
15. Wolff SD, Schwitter J, Coulden R, et al. Myocardial first-pass perfusion magnetic resonance imaging: a multicenter dose-ranging study. Circulation 2004;110:732–7. [PubMed: 15289374]
16. Gould KL. Quantification of coronary artery stenosis in vivo. Circ Res 1985;57:341–53. [PubMed: 3896552]
17. Pijls NH, De Bruyne B, Peels K, et al. Measurement of fractional flow reserve to assess the functional severity of coronary-artery stenoses. N Engl J Med 1996;334:1703–8. [PubMed: 8637515]

18. Panting JR, Gatehouse PD, Yang GZ, et al. Abnormal subendocardial perfusion in cardiac syndrome X detected by cardiovascular magnetic resonance imaging. N Engl J Med 2002;346:1948–53. [PubMed: 12075055]

19. Wang L, Jerosch-Herold M, Jacobs DR Jr, Shahar E, Folsom AR. Coronary risk factors and myocardial perfusion in asymptomatic adults: the Multi-Ethnic Study of Atherosclerosis (MESA). J Am Coll Cardiol 2006;47:565–72. [PubMed: 16458137]

20. Doyle M, Fuisz A, Kortright E, et al. The impact of myocardial flow reserve on the detection of coronary artery disease by perfusion imaging methods: an NHLBI WISE study. J Cardiovasc Magn Reson 2003;5:475–85. [PubMed: 12882078]

21. Di Carli MF, Janisse J, Grunberger G, Ager J. Role of chronic hyperglycemia in the pathogenesis of coronary microvascular dysfunction in diabetes. J Am Coll Cardiol 2003;41:1387–93. [PubMed: 12706936]

22. Yokoyama I, Momomura S, Ohtake T, et al. Improvement of impaired myocardial vasodilatation due to diffuse coronary atherosclerosis in hypercholesterolemics after lipid-lowering therapy. Circulation 1999;100:117–22. [PubMed: 10402439]

23. Parkash R, deKemp RA, Ruddy TD, et al. Potential utility of rubidium 82 PET quantification in patients with 3-vessel coronary artery disease. J Nucl Cardiol 2004;11:440–9. [PubMed: 15295413]

24. Hachamovitch R, Berman DS, Shaw LJ, et al. Incremental prognostic value of myocardial perfusion single photon emission computed tomography for the prediction of cardiac death. Differential stratification for risk of cardiac death and myocardial infarction. Circulation 1998;97:535–43. [PubMed: 9494023]

25. Hachamovitch R, Hayes SW, Friedman JD, Cohen I, Berman DS. Comparison of the short-term survival benefit associated with revascularization compared with medical therapy in patients with no prior coronary artery disease undergoing stress myocardial perfusion single photon emission computed tomography. Circulation 2003;107:2900–7. [PubMed: 12771008]

26. Sorajja P, Chareonthaitawee P, Rajagopalan N, et al. Improved survival in asymptomatic diabetic patients with high-risk SPECT imaging treated with coronary artery bypass grafting. Circulation 2005;112:I311–6. [PubMed: 16159837]

27. Selvanayagam JB, Jerosch-Herold M, Porto I, et al. Resting myocardial blood flow is impaired in hibernating myocardium. A magnetic resonance study of quantitative perfusion assessment. Circulation 2005;112:3289–96. [PubMed: 16286587]

28. Selvanayagam JB, Cheng ASH, Jerosch-Herold M, et al. Effect of distal embolization on myocardial perfusion reserve after percutaneous coronary intervention: a quantitative magnetic resonance perfusion study. Circulation 2007;116:1458–64. [PubMed: 17785626]

29. Gatehouse PD, Elkington AG, Ablitt NA, Yang GZ, Pennell DJ, Firmin DN. Accurate assessment of the arterial input function during high-dose myocardial perfusion cardiovascular magnetic resonance. J Magn Reson Imaging 2004;20:39–45. [PubMed: 15221807]

30. Cheng AS, Pegg TJ, Karamitsos TD, et al. Cardiovascular magnetic resonance perfusion imaging at 3-tesla for the detection of coronary artery disease: a comparison with 1.5-tesla. J Am Coll Cardiol 2007;49:2440–9. [PubMed: 17599608]

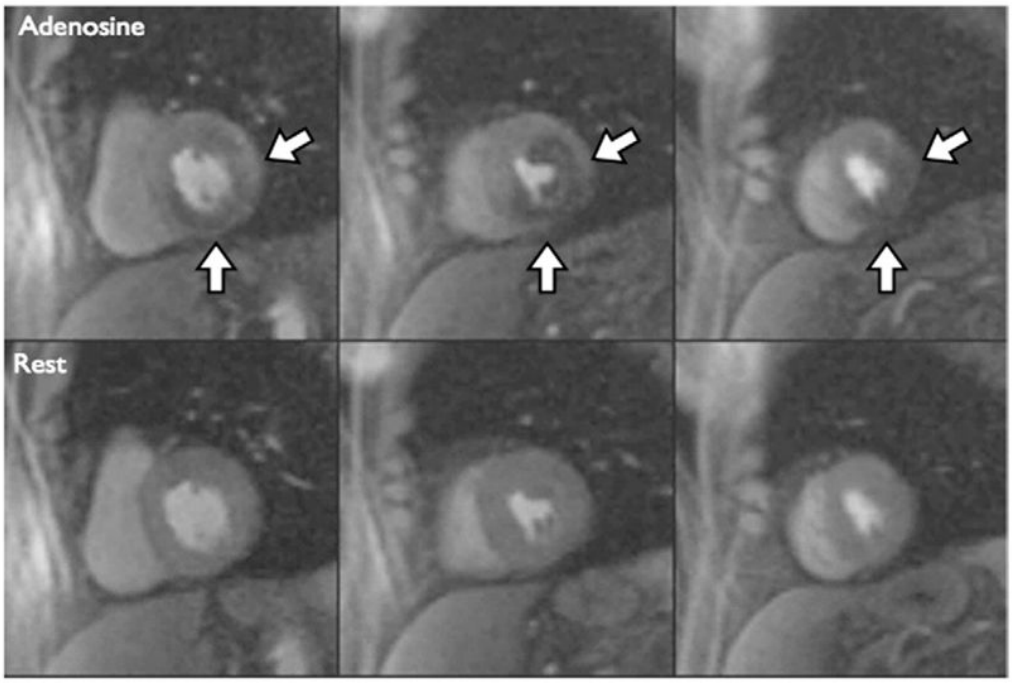

Figure 1. Qualitative Interpretation of Perfusion CMR Imaging

First-pass perfusion images obtained during peak contrast enhancement cardiac magnetic resonance (CMR) imaging of the basal left ventricular **(left column)**, mid-ventricular **(middle column)**, and apical **(right column)** slices are shown during hyperemic **(top row)** and resting **(bottom row)** conditions. The **white arrows** point to a large perfusion defect extending from the basal to the apical slice.

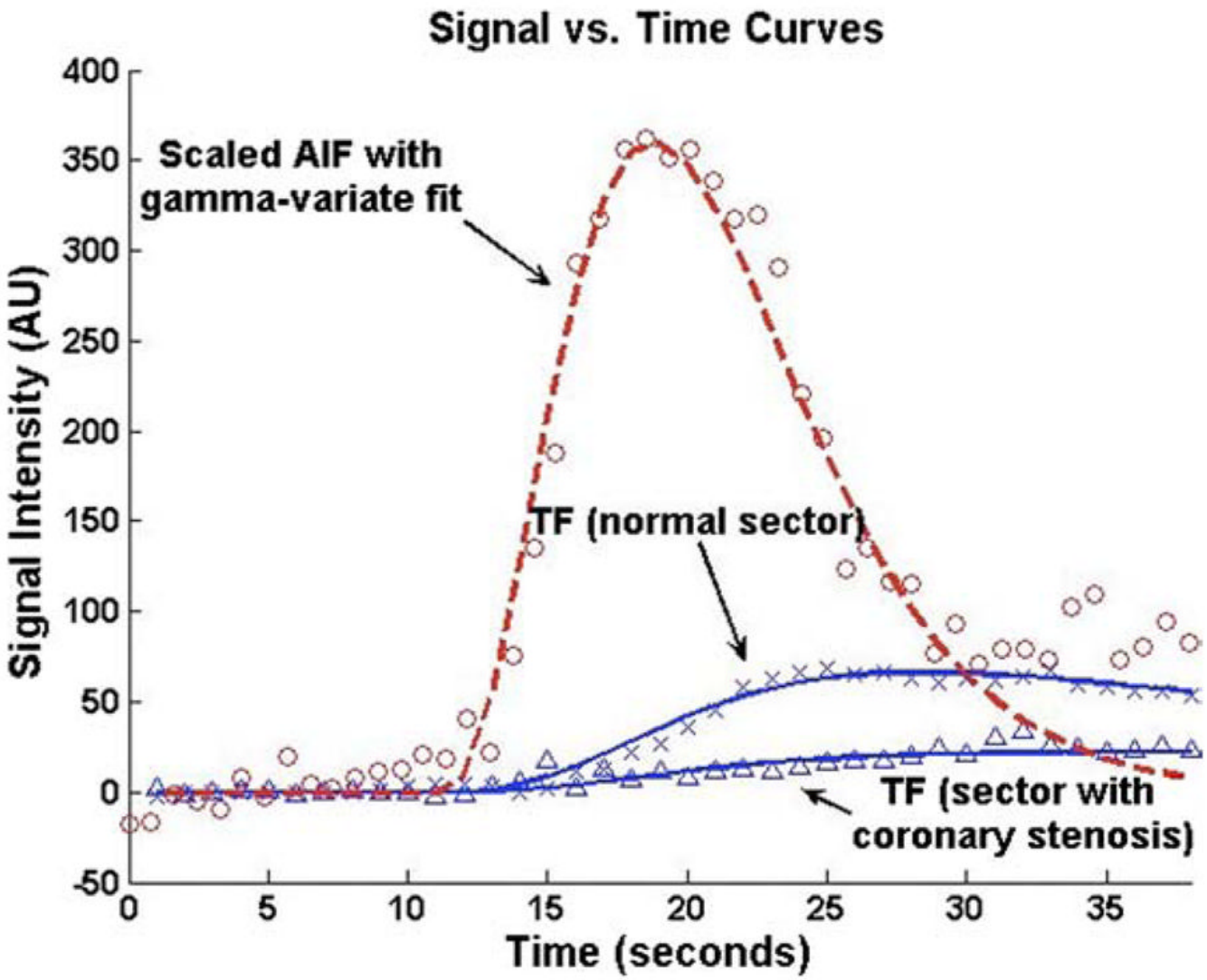

Figure 2. Perfusion Time Intensity Curves

Representative time intensity curves used for Fermi function deconvolution are shown. The **red line and circles** represent a typical arterial input function (AIF). The **top blue line and Xs** represent the tissue function (TF) in a segment supplied by a coronary artery without a stenosis. The **bottom blue line and triangles** represent the tissue function in a segment supplied by a stenosed coronary artery.

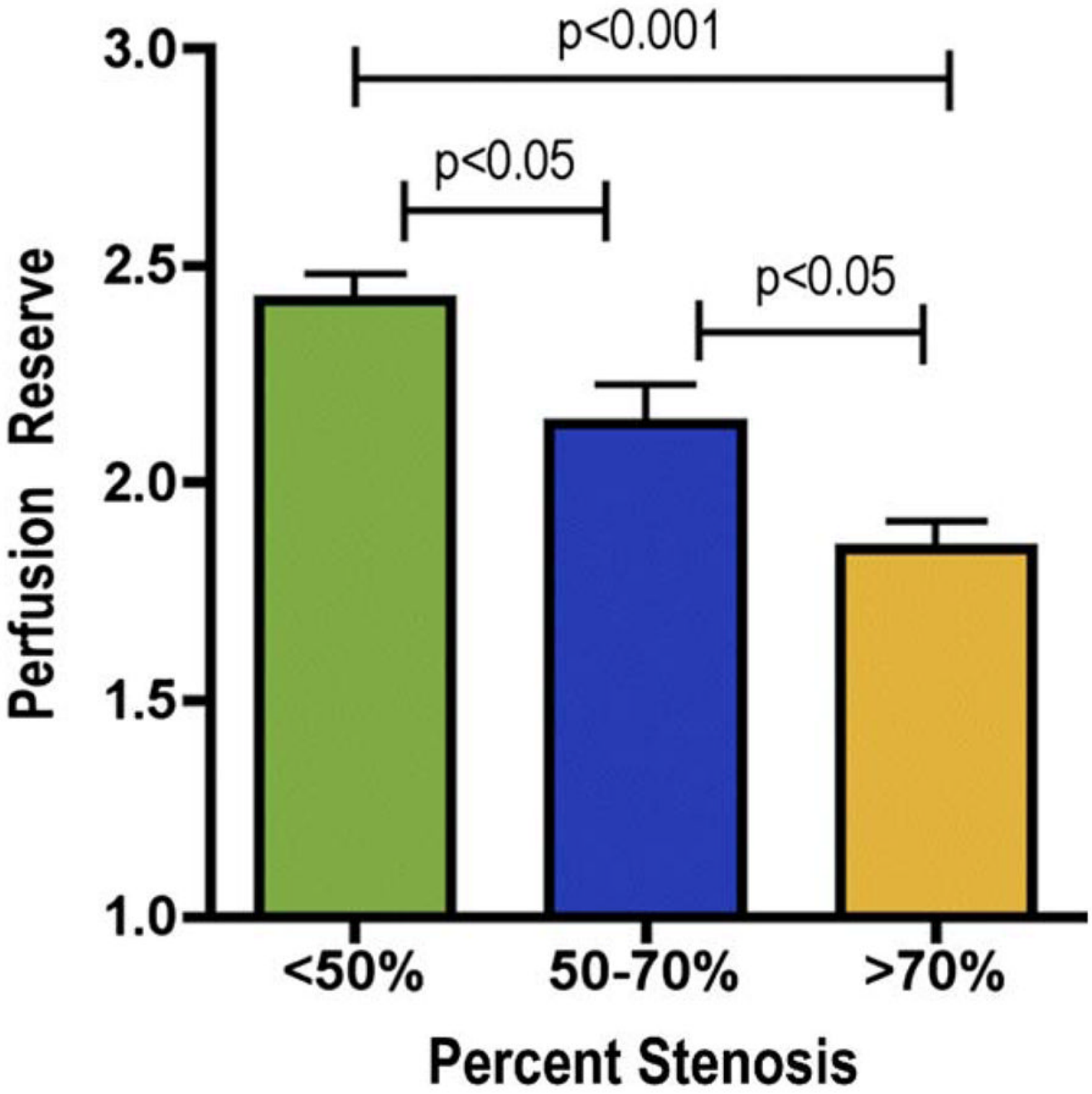

Figure 3. Relationship Between Perfusion Reserve and Percent Stenosis

Segmental perfusion reserve (mean ± SE) decreases in a stepwise manner as the severity of coronary stenosis increases.

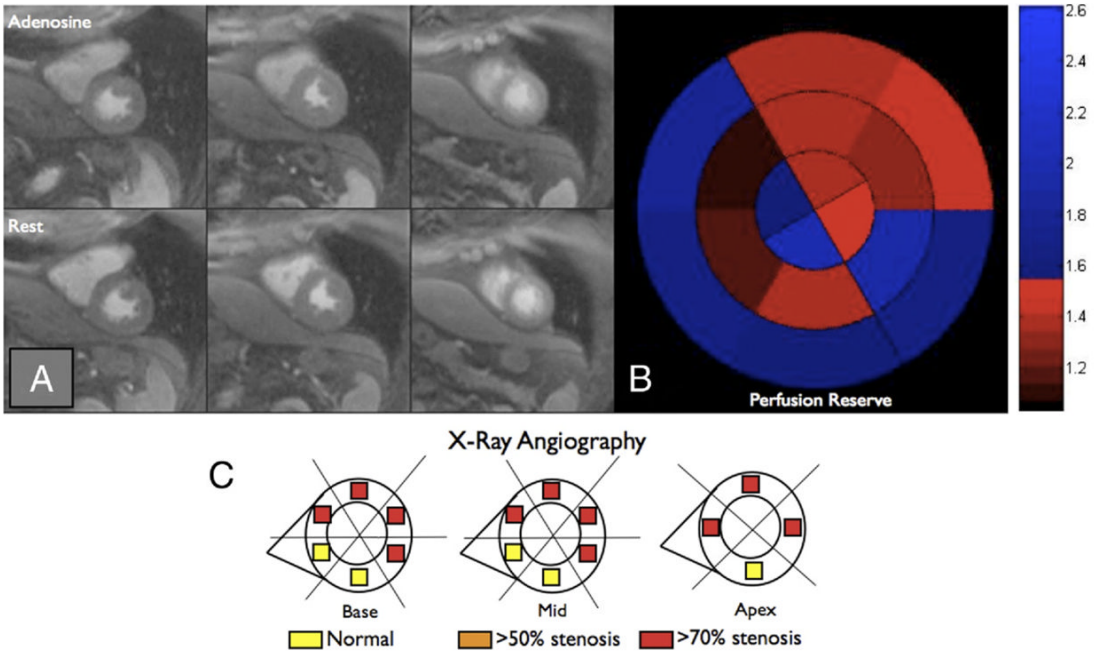

Figure 4. Comparison of Qualitative Interpretation and Perfusion Reserve Analysis, Example 1

(A) No perfusion defects are visually appreciated on first-pass perfusion images obtained during peak contrast enhancement of the basal left ventricular **(left column)**, the mid-ventricular **(middle column)**, and the apical **(right column)** slices during hyperemic **(top row)** or resting **(bottom row)** conditions. **(B)** Measured perfusion reserve for each of the 16 segments is plotted using a bulls-eye graph with the color scale shown on the **right**. Fifty-six percent of the left ventricle had a perfusion reserve <1.55. **(C)** Based on quantitative coronary angiography, each of the 16 segments was determined to be supplied by a stenosis <50% **(yellow)**, >50% **(orange)**, or >70% **(red)**. Despite the absence of a visually appreciable perfusion defect, an abnormal perfusion reserve was present in this patient with multivessel coronary artery disease.

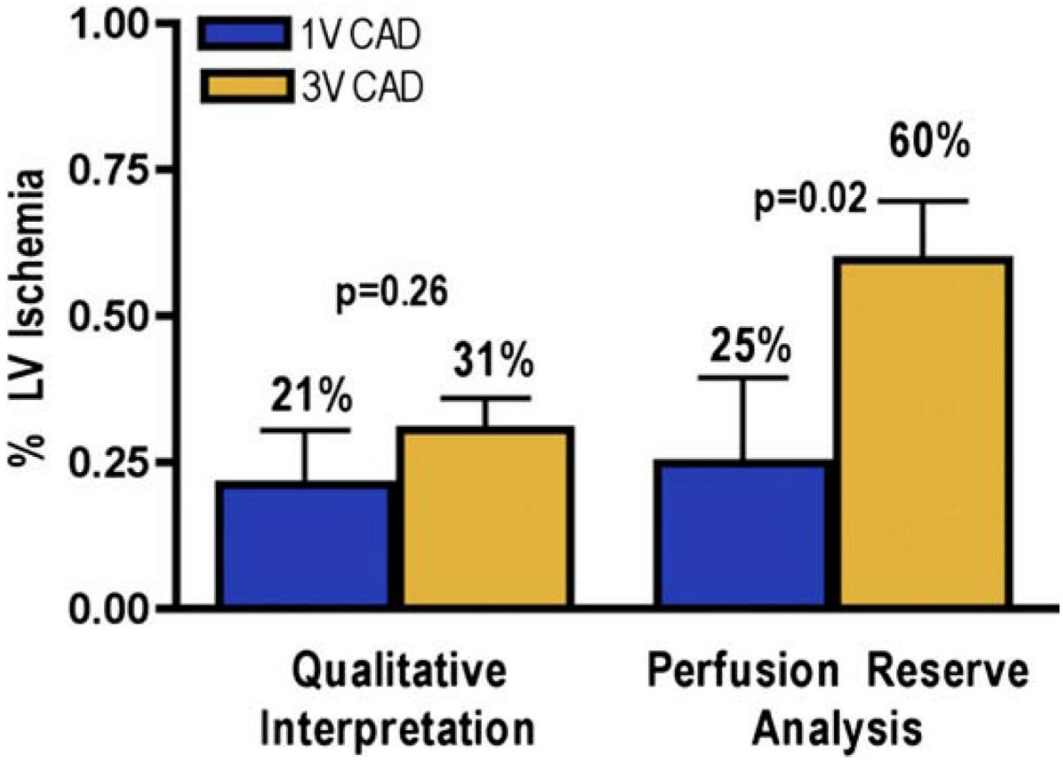

Figure 5. Assessment of LV Ischemic Burden

Comparison of qualitative interpretation and perfusion reserve analysis: unlike perfusion reserve analysis, qualitative interpretation cannot detect the difference in ischemic burden (percent left ventricular [LV] ischemia [mean ± SE]) that is present in patients with single-vessel (1V) coronary artery disease (CAD) **(blue bars)** or triple-vessel (3V) CAD **(gold bars)**.

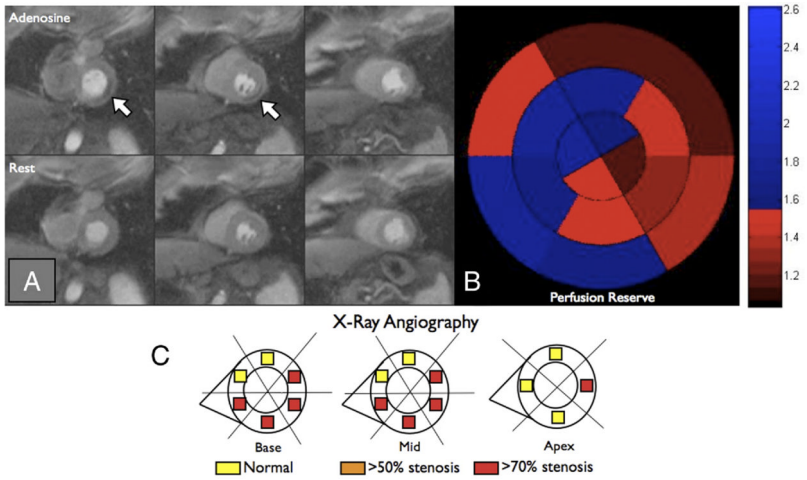

Figure 6. Comparison of Qualitative Interpretation and Perfusion Reserve Analysis, Example 2

(A) First-pass perfusion images obtained during peak contrast enhancement of the basal left ventricular slice **(left column)**, the mid-ventricular slice **(middle column)**, and the apical slice **(right column)** are shown during hyperemic **(top row)** and resting **(bottom row)** conditions. The **white arrows** point to a small perfusion defect in the inferolateral wall. **(B)** Perfusion reserve for each of the 16 segments is plotted using a bulls-eye graph with the color scale shown on the **right**. Fifty-six percent of the left ventricle had a perfusion reserve <1.55. **(C)** Based on quantitative coronary angiography, each of the 16 segments was determined to be supplied by a stenosis <50% **(yellow)**, >50% **(orange)**, or >70% **(red)**. Qualitative interpretation significantly underestimated the ischemic burden in this patient with multivessel coronary artery disease.

Table 1

Patient Characteristics

Male, n (%)	28 (68)
Age, yrs	68 ± 12
Body mass index, kg/m^2	30.2 ± 4.8
Symptoms, n (%)	38 (93)
Chest pain	32 (78)
Shortness of breath	4 (10)
Other symptoms	2 (5)
None	3 (7)
History of myocardial infarction, n (%)	14 (34)
Previous revascularization, n (%)	12 (29)
Diabetes mellitus, n (%)	11 (27)
Prior tobacco use, n (%)	27 (66)
Dyslipidemia, n (%)	36 (88)
Hypertension, n (%)	34 (83)
Medications, n (%)	
Aspirin	33 (80)
Beta-blockers	22 (54)
Angiotensin-blockers	20 (49)
Statins	28 (68)
Nitrates	14 (34)
Hemodynamics	
Peak systolic blood pressure, mm Hg	137 ± 27
Peak diastolic blood pressure, mm Hg	73 ± 13
Peak heart rate, beats/min	87 ± 16
Cardiac magnetic resonance data	
Left ventricular ejection fraction, %	58 ± 11
Left ventricular end-diastolic volume, ml	141 ± 37
Left ventricular end-systolic volume, ml	62 ± 31
Left ventricular mass, g	132 ± 38
Late gadolinium enhancement, n (%)	18 (44)
Coronary angiography, n (%)	
Any stenoses >50%	29 (71)
1-vessel disease	11 (27)
2-vessel disease	3 (7)

3-vessel disease	15 (37)